AD-A138 579 TEST AND EVALUATION OF THE RADAR THUNDERSTORM TURBULENCE DETECTION SYSTEM..(U) FEDERAL AVIATION ADMINISTRATION TECHNICAL CENTER ATLANTIC CIT.. 1/1

UNCLASSIFIED W LEWIS ET AL. JUL 82 DOT/FAA/CT-82/6 F/G 4/2 NL

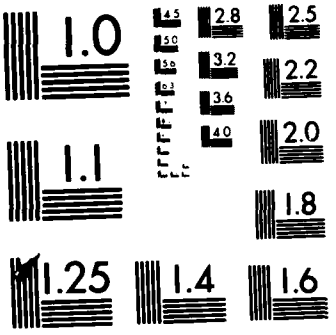

DOT/FAA/RD-82/22
DOT/FAA/CT-82/6

TEST AND EVALUATION OF THE RADAR THUNDERSTORM TURBULENCE DETECTION SYSTEM (PHASE I)

William Lewis
Robert G. Oliver
Alfred DeLaMarche
Tai Y. Lee

Prepared By
FAA Technical Center
Atlantic City Airport, N.J. 08405

July 1982

Interim Report

U.S Department of Transportation
Federal Aviation Administration
Systems Research & Development Service
Washington, D.C. 20590

Technical Report Documentation Page

1. Report No.	2. Government Accession No.	3. Recipient's Catalog No.
DOT/FAA/RD-82/22	AD-A138579	

4. Title and Subtitle
TEST AND EVALUATION OF THE RADAR THUNDERSTORM TURBULENCE DETECTION SYSTEM (PHASE I)

5. Report Date
July 1982

6. Performing Organization Code
ACT-100

7. Author(s)
William Lewis, Robert G. Oliver, Alfred DeLaMarche, and Tai Y. Lee

8. Performing Organization Report No.
DOT/FAA/CT-82/6

9. Performing Organization Name and Address
Federal Aviation Administration
Technical Center
Atlantic City Airport, New Jersey 08405

10. Work Unit No. (TRAIS)

11. Contract or Grant No.
156-230-510

12. Sponsoring Agency Name and Address
U.S. Department of Transportation
Federal Aviation Administration
Systems Research and Development Service
Washington, D.C. 20590

13. Type of Report and Period Covered
Interim Report
March 1980 - June 1981

14. Sponsoring Agency Code

15. Supplementary Notes

16. Abstract

A thunderstorm turbulence detection test bed was developed at the Federal Aviation Administration (FAA) Technical Center by the Massachusetts Institute of Technology, Lincoln Laboratory. This consists of a system to measure and process Doppler radar parameters, and an FAA aircraft instrumented to measure turbulence concurrently with the radar observations. The test bed is being used to investigate the relationship between radar- and aircraft-measured turbulence.

Radar measurements of the Doppler spectrum width and aircraft measurements of airspeed fluctuations and center-of-gravity normal accelerations were converted to $\epsilon^{1/3}$ (cube root of the turbulence dissipation factor) for comparison.

Several data collections were made during the summer of 1980. Results of data analysis showed that the major turbulence sequences experienced by the aircraft were essentially reflected by the radar. However, linear correlation coefficients between radar and aircraft $\epsilon^{1/3}$ were only about 0.5. The low correlations are considered to be due to differences in response to turbulence by the two measuring systems, deficiencies in the radar processing, and radar data interpolation errors between the 80-second radar scans. In a more practical analysis, radar-measured turbulence, classified into ranges of light, moderate, and severe turbulence, showed a potentially useful relationship to aircraft turbulence. The predictive value was enhanced by consideration of radar reflectivity factor as a screening variable.

17. Key Words	18. Distribution Statement
Turbulence, Thunderstorms, Aircraft Turbulence, Doppler Weather Radar, Airport Surveillance Radar, Air Traffic Turbulence Advisories	This document is available to the U.S. public through the National Technical Information Service, Springfield, Virginia 22161

19. Security Classif. (of this report)	20. Security Classif. (of this page)	21. No. of Pages	22. Price
Unclassified	Unclassified	29	

TABLE OF CONTENTS

A1

LIST OF ILLUSTRATIONS

LIST OF TABLES

INTRODUCTION

PURPOSE.

The purpose of this project is to determine if a pulse Doppler radar can detect the turbulence associated with thunderstorms and provide turbulence warnings to aircraft in airport terminal areas.

BACKGROUND.

Thunderstorms are a major problem to the safe and efficient movement of aircraft. Inadequate warning of thunderstorm hazards often results in aircraft encountering dangerous conditions. In attempts to avoid the hazards, en route aircraft are sometimes diverted hundreds of miles, while in terminal areas landings and take-offs are delayed. This causes disruptions in operations and increases fuel and other costs.

Some information on thunderstorm hazards is presently available through radar measurements of precipitation intensity. However, after many years of research, conducted primarily by the National Severe Storms Laboratory (NSSL) (references 1 and 2), it has been determined that precipitation intensity alone cannot be relied on to identify turbulent areas. Rather, the research showed that the degree of turbulence in a thunderstorm is related to the peak precipitation intensity of the storm. However, the turbulence may occur anywhere in the storm area. Thus, to insure avoiding heavy turbulence, strong storms should be avoided entirely. This is a sound procedure but does deny use of large amounts of airspace, much of it nonhazardous.

Doppler radar techniques offer the potential for determining where turbulent areas are in thunderstorms through measurement of precipitation particle movement. The most promising means is by measurement of the Doppler velocity variance which is related to small-scale wind variability, i.e., turbulence within a range-azimuth cell (pulse volume). The mean Doppler velocity which shows large-scale wind variability from pulse volume to pulse volume, may also be related to the production of turbulence. Finally, the precipitation intensity, i.e., radar reflectivity factor, provides a measure of overall storm intensity and reliably identifies damaging hail (reference 3).

The Federal Aviation Administration (FAA) Systems Research and Development Service (SRDS) is sponsoring a research program to investigate the use of a pulse Doppler radar in detecting thunderstorm turbulence. The Massachusetts Institute of Technology (MIT) Lincoln Laboratory, through Interagency Agreement DTFA01-80-Y-10546, is part of this effort. This research program is part of a larger program jointly sponsored by the Departments of Commerce, Defense, and Transportation (DOC, DOD, DOT) to develop the next generation weather radar (NEXRAD) system. NEXRAD is expected to satisfy most of the thunderstorm-related hazardous weather warning requirements of the various government agencies.

Lincoln Laboratory has cooperated in the establishment of a test bed at the FAA Technical Center, Atlantic City Airport, New Jersey. This consists of a pulse Doppler radar and peripheral equipment to observe, process, display, and record the Doppler information, and an instrumented aircraft to measure and record turbulence concurrently with the radar observations.

This report describes the test bed, the radar and aircraft turbulence measurements, and presents results from the 1980 data collection.

SYSTEM DESCRIPTION.

The turbulence measurement instrumentation block diagram is shown in figure 1. The system is installed in the Technical Center's Terminal Facility for Automation and Surveillance Testing (TFAST).

The pulse Doppler instrumentation radar uses one channel of a standard dual channel Airport Surveillance Radar (ASR)-8. A parabolic 15-foot pencil-beam antenna (figure 2) is interconnected through a waveguide switching arrangement which allows the ASR-8 to operate with either its standard search antenna or the pencil-beam antenna. In this latter configuration, peak power is 1 megawatt, frequency 2790 megahertz (MHz), pulse repetition frequency (PRF) 1030 pulses per second (pps), pulse length 0.6 microsecond (μs), and one-way antenna beam width 1.6°.

The station-keeping radar is a standard ASR-7 airport terminal radar. Associated with it is an Air Traffic Control Radar Beacon System (ATCRBS) equipped with a beacon decoder that provides the test aircraft's position to the NOVA computer. The ASR-7/ATCRBS antennas are shown in figure 2. The ASR-7 and beacon information is shown on two displays. One is associated with the air traffic control AN/TPX-42 system and shows beacon targets with altitude and identity tags. The second is the Data Entry and Display System (DEDS) which shows the beacon track of the test aircraft and a wedged-shaped data window from the pulse-Doppler instrumentation radar. The approximately 10 x 10-nautical mile (nmi) data window is configured in a thunderstorm area and the instrumented aircraft directed to fly through it.

Fields of precipitation intensity (radar reflectivity factor in terms of dBZ), Doppler mean velocity, and velocity variance in terms of $\epsilon^{1/3}$ (cube root of the turbulence dissipation factor (discussed later) may be displayed in the window independently or collectively. These values are used to help select areas for data collection and to reject areas likely to be too hazardous. Both the AN/TPX-42 and the DEDS displays show any two of six levels (contours) of precipitation intensity processed from the ASR-7 signals (reference 4). The precipitation contours are used to select thunderstorms for data collection. (For the 1981 season, the video integrator and processor (VIP) contours were remoted from the local National Weather Service WSR-57 radar.)

The radar controller unit was designed and built by Lincoln Laboratory. It generates triggers, gates, and pulses for the radars and beacon transmitter. It controls the size of the data window, generates commands to the two 10-bit analog to digital converters (A/D's) to digitize the inphase (I) and quadrature (Q) signals and controls their transmission to the buffer memory. Periodic interrupt commands are sent to the NOVA to signal when data taking commences and ceases.

The buffer memory, also designed and built by Lincoln Laboratory, has a capacity of 262,144 twenty-one bit words. It is filled with A/D output data as the antenna sweeps the window. The antenna rotation rate is 1 revolution per minute (rpm), which, for a PRF of 1030 pps, is 0.006° per pulse. About 200 pulses are used for each range gate resulting in an azimuthal resolution of 1.2° (two-way beamwidth). The number of range gates per azimuth interval (1.2°) can be set to 12, 28, 60, 124, or 252, depending on window dimensions desired. A setting of 12 provides a narrow range span over a wide azimuth swath (many 1.2° intervals), while a setting

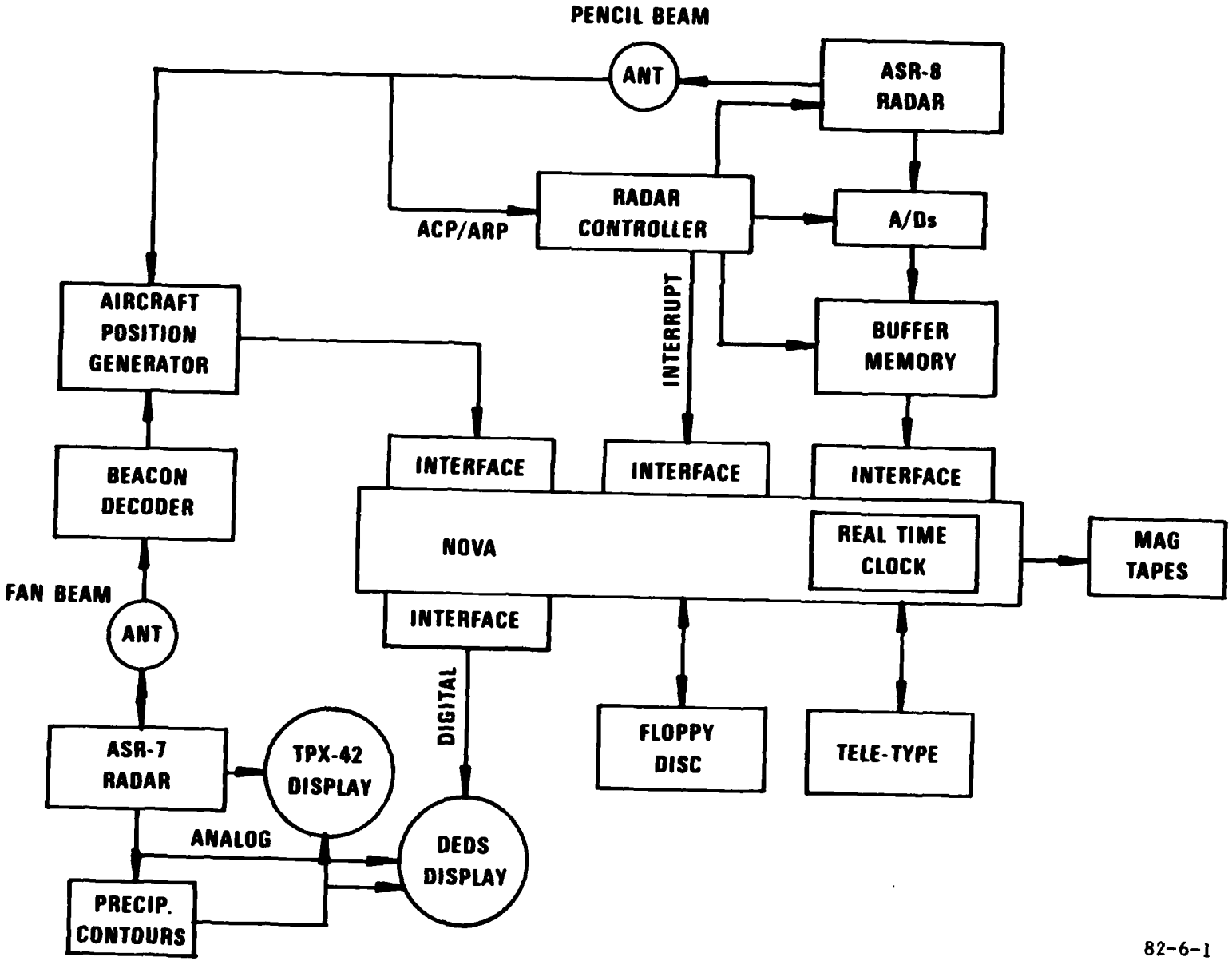

FIGURE 1. TURBULENCE MEASUREMENT SYSTEM

FIGURE 2. ASR AIR TRAFFIC CONTROL AND TURBULENCE ANTENNAS

of 252 provides the reverse. Usual settings are 28 and 60. Range gate samples can be taken every 750, 1500, or 3000 nanoseconds (ns) (112.5, 225, or 450 meters). The window expands in range as the range gate spacing increases. Normally, the 3000 ns spacing is selected since it provides acceptable data point resolution and ample window size.

After the antenna sweeps the window, the radar controller unit returns the antenna to the original position (or a new one) to await another sweep command. The NOVA 1200 computer then orders the transmission of radar digital messages from the buffer memory to the magnetic tapes. Aircraft beacon reports are also processed, digitized, and stored on tape. The fields of radar reflectivity factor, Doppler mean velocity, and $\epsilon^{1/3}$ are generated by the NOVA for display in the window. Cycling time between scans is normally about 80 seconds.

The data are recorded on Data General model 6021 nine-track magnetic tapes. The tapes are standard 800 bits per inch (bpi) recorded on at a rate of 75 inches per second. Approximately 15 minutes of data can be recorded on each tape.

The floppy disc is a Data General dual system used for recording and entering software.

The teletype is a Tektronics display terminal model 4014-1. This provides both cathode ray tube (CRT) and typewriter interface with the NOVA computer. Recording and control equipment are shown in figure 3.

AIRCRAFT EQUIPMENT.

A Grumman Gulfstream-I twin-engine turboprop aircraft (figure 4) was instrumented to provide data for turbulence measurements. Instruments and data rates are:

1. Altitude transducer (1/sec)
2. Differential Pitot pressure (airspeed) transducer (100/sec)
3. Air temperature (1/sec)
4. Center-of-gravity (CG) accelerometer (20/sec)
5. Litton Inertial Navigation System (INS) latitude/longitude (1/sec)
6. Crystal-controlled clock (1/sec)

The data are recorded in the aircraft on a Kennedy model 9832 digital tape recorder.

CALIBRATION.

The beacon antenna azimuth accuracy was determined by observing a ground transponder at a known location. The instrumentation radar pointing accuracy (azimuth and elevation) was determined by automatically directing the antenna to an accurately computer calculated position of the sun. By noting how far the antenna had to be moved to be precisely on boresight with the sun, it was found that the error was less than 0.1°. Boresighting was achieved by sensing the peak solar thermal noise level with an root mean square (rms) voltmeter. The antenna gain was determined by measuring the solar flux level and comparing it with known (published) values. The radar receiver gain was determined by injecting a calibrated noise signal into the waveguide directional coupler.

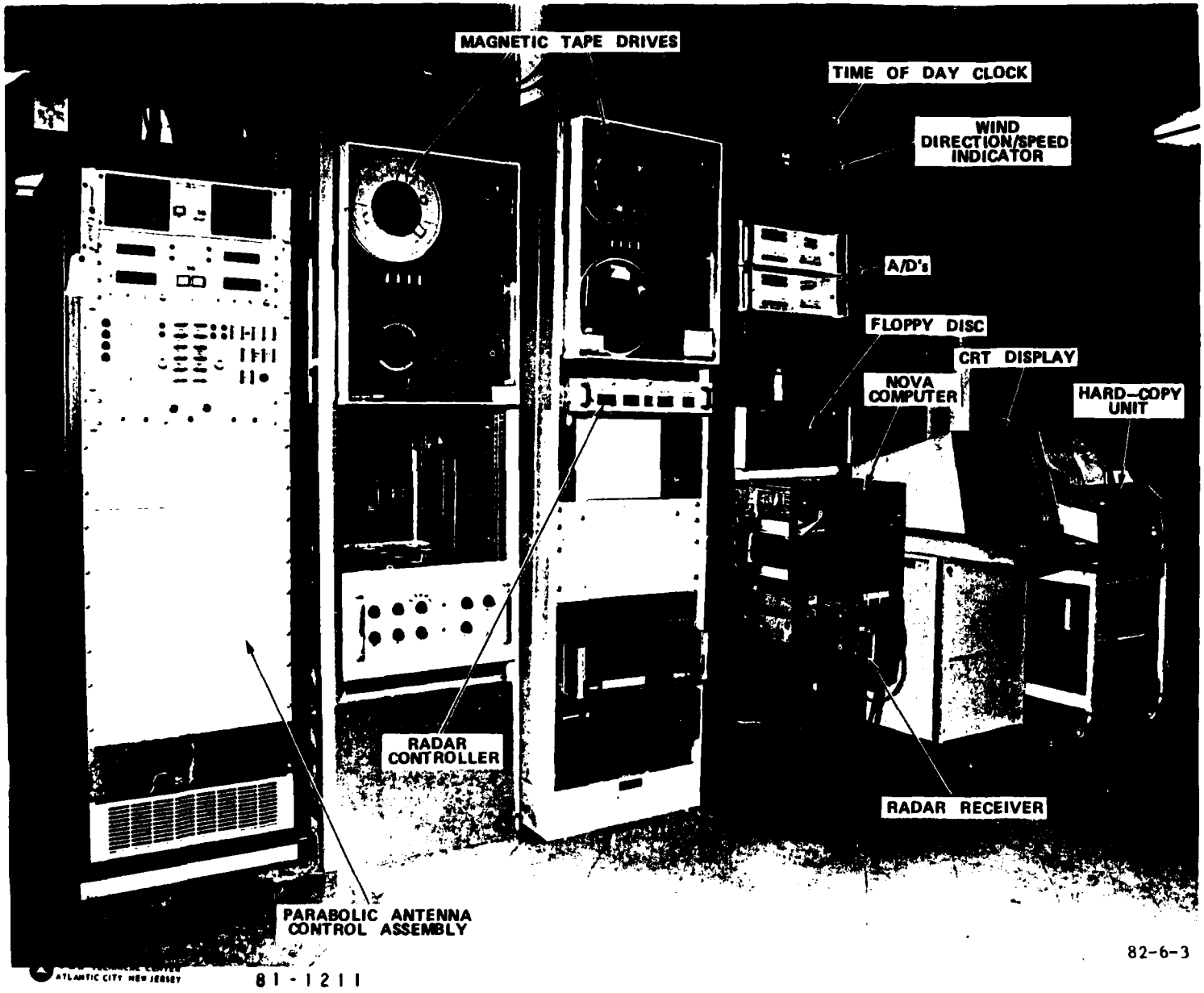

FIGURE 3. TURBULENCE TE T BED RECORDING AND CONTROL EQUIPMENT

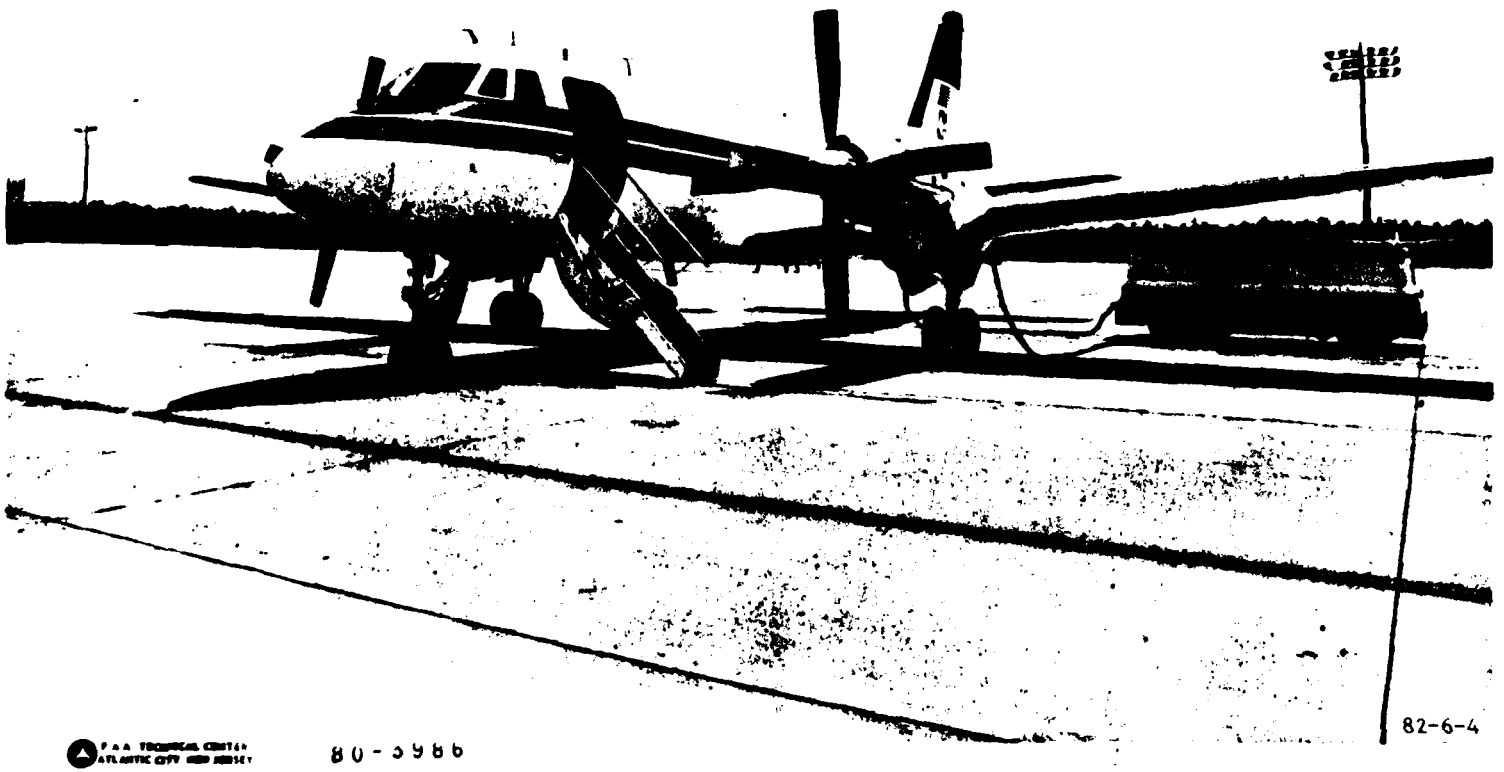

FIGURE 4. GRUMMAN GULFSTREAM - I TEST AIRCRAFT

The ground and aircraft instrument clocks were carefully synchronized before takeoff, and rechecked occasionally during flights. Timing accuracy is within 1 second which is well within acceptable limits.

DATA COLLECTION AND ANALYSIS

GENERAL.

The aircraft was launched when thunderstorms were occurring within 40 nmi of the radar (40 nmi is the practical limit for adequate pulse volume resolution with the instrumentation radar). The National Weather Service WSR-57 radar VIP level 3 and 4 storms (41 to 46 dBZ heavy and 46 to 50 dBZ very heavy, respectively) were preferred. VIP level 5 and 6 storms were avoided because of the high probability of damaging hail.

The aircraft was flown in an altitude block of 3,000 to 5,000 feet mean sea level (m.s.l.) to avoid encroaching on the New York Air Route Traffic Control Center airspace. This facilitated aircraft movements which were coordinated with the Atlantic City Airport and adjacent approach control jurisdictions by an assigned air traffic controller.

The instrumentation radar window was placed in the storm of interest and the aircraft directed to fly on paths that would intercept high values of $\epsilon^{1/3}$ (turbulence measurement). The altitude of the window was set at window midrange to coincide with the aircraft's planned flight altitude (usually 4,000 feet). Occasionally, radar data were taken 1,000 feet above and below the mean altitude to obtain vertical shear information.

RADAR MEASUREMENTS.

Raw radar I and Q components for each range-azimuth cell (pulse-volume) in the data window were recorded range sequentially. These were then reordered in azimuth, and a maximum entropy estimation of the autocorrelation lags made for each pulse-volume using 204 I and Q components. The autocorrelation lags were used to compute the precipitation intensity (radar reflectivity factor, dBZ), mean velocity, and velocity variance through specific pulse pair algorithms (reference 5).

In the pulse-volume, the scatterers are assumed to be carried by a homogenous turbulent atmosphere with a Gaussian velocity distribution and radar spectrum. The radar antenna beam shape is also approximately Gaussian.

The radar reflectivity factor is determined from the individual signal values of the 204 pulses. The mean velocity is determined from signal differences between successive pulse pairs (1-2, 2-3, etc.). The velocity variance is determined from signal differences between alternate pulse pairs (1-3, 3-5, etc.).

The algorithms require a minimum signal-to-noise (S/N) value. In particular, the 2nd moment S/N estimator requires at least a 3 decibel (dB) S/N ratio.

The mean velocity and velocity variance estimates from pulse-pair processing are most accurate with narrow spectrum widths. Standard errors increase exponentially with broader spectra. Also, nonsymmetric (non-Gaussian) spectra produce errors. (These inaccuracies are discussed in reference 6.)

The velocity variance, σ_v^2, is related to the dissipation factor, ϵ, by the following equation (reference 5):

$$\sigma_v^2 = 1.828(\epsilon a)^{2/3} \quad (1)$$

where,

σ_v^2 = velocity variance (cm^2/sec^2)

ϵ = dissipation factor (cm^2/sec^3)

a = two-way Gaussian half-beam width (centimeters (cm))

1.828 = known constants (assuming isotropic and homogenous turbulence)

Thus,

$$\epsilon_r^{1/3} = \frac{\sigma_v}{1.352\ a^{1/3}} \ (cm^{2/3}\ sec^{-1}) \quad (2)$$

where,

σ_v = is the Doppler spectrum width.

Since "a" is a function of range, $\epsilon^{1/3}$ is essentially a range-weighted spectrum width and, as such, should be superior to spectrum width as a turbulence measure.

The dissipation factor (reference 7) represents the kinetic energy converted to heat per unit mass per unit time as larger eddies decay into progressively smaller eddies. The system is steady-state in the inertial subrange (wavelengths about 1 cm to 1 kilometer (km)) where atmospheric motions are isotropic. Most gusts which produce turbulence in aircraft are included within this range. $\epsilon^{1/3}$ rather than ϵ is used as a turbulence measure because it is directly proportional to the rms vertical acceleration experienced by an aircraft (reference 7) as well as to the Doppler spectrum width (equation 2).

Equation 2 is valid for the inertial subrange if the turbulence is isotropic and homogeneous within a pulse volume, the raindrops move with the wind and there is no wind shear. Except for wind shear, these conditions were substantially met by restricting measurement range and observing at low elevation angles. Wind shear broadening of spectrum width can, in principle, be removed by measuring the mean velocity in adjacent pulse volumes and subtracting out the effect.

Aircraft beacon data were processed by a fast Fourier transform (FFT) smoothing and interpolation technique to provide position points at 1.2-second intervals. The radar data fields were also smoothed and interpolated by a two-dimensional FFT procedure, then merged with the aircraft data to provide radar values at the aircraft position points. Figures 5 and 6 show contour plots of $\epsilon^{1/3}$ and radar reflectivity factor (dBZ), respectively, with the aircraft track superimposed. The

midpoint of the track is the aircraft position at scan time. The tracks, which extend back 40 seconds to the previous scan and forward 40 seconds to the next scan, are adjusted to allow for mean radar pattern movement between scans. The much more structured nature of the turbulence pattern relative to the reflectivity pattern is evident from an inspection of figures 5 and 6.

AIRCRAFT MEASUREMENTS.

Three measures of turbulence were derived from the aircraft instrumentation:

1. Derived equivalent gust velocity (reference 8)

$$U_{de} = \frac{2\Delta a_N W}{C_{L_\alpha} \rho_o K_g V_e S} \ (ms^{-1}) \qquad (3)$$

where,

Δa_N = incremental normal acceleration

W = aircraft weight

C_{L_α} = wing lift curve slope

ρ_o = air density at sea level

K_g = gust alleviation factor

V_e = equivalent airspeed

S = wing area

U_{de} is based on unsteady lift theory and has been used by aircraft designers to predict maximum acceleration to be expected from vertical gusts.

U_{de} values were computed each 0.1 second from two preaveraged accelerations. The peak value (positive or negative) was extracted each second for running 7-second periods.

2. $\epsilon_a^{1/3}$ from the center-of-gravity accelerometer (reference 5)

$$\epsilon_a^{1/3} = \frac{\sqrt{3D_a}\ M\ V^{3/4}}{C_{L_\alpha} S\ C^{1/2} \rho} \ (cm^{2/3} sec^{-1}) \qquad (4)$$

where,

D_a = acceleration structure function — average of the square of differences between successive acceleration measurements (homogeneous isotropic turbulence assumed).

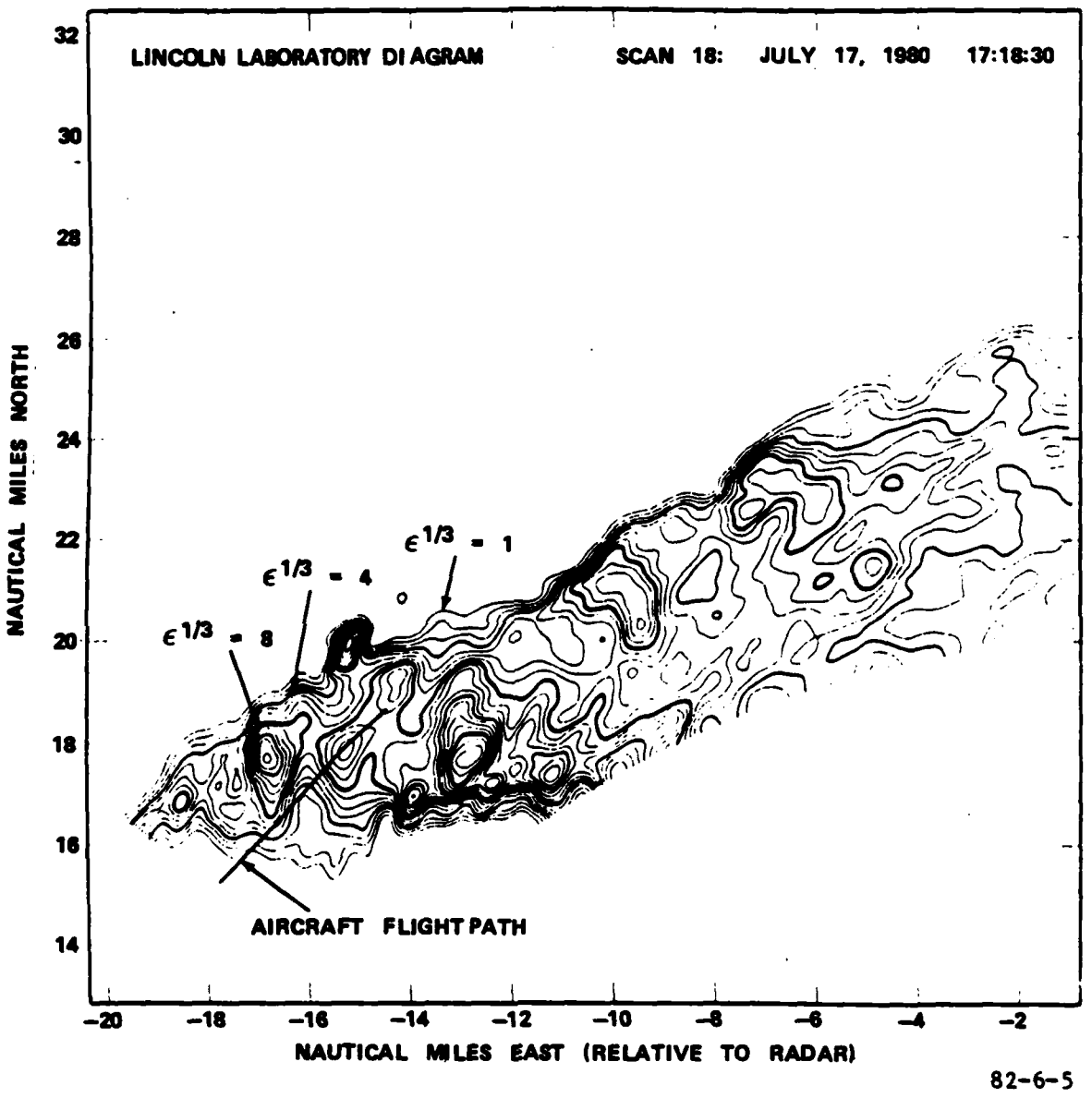

FIGURE 5. RADAR $\epsilon^{1/3}$ CONTOURS IN UNITY STEPS ($cm^{2/3}sec^{-1}$)

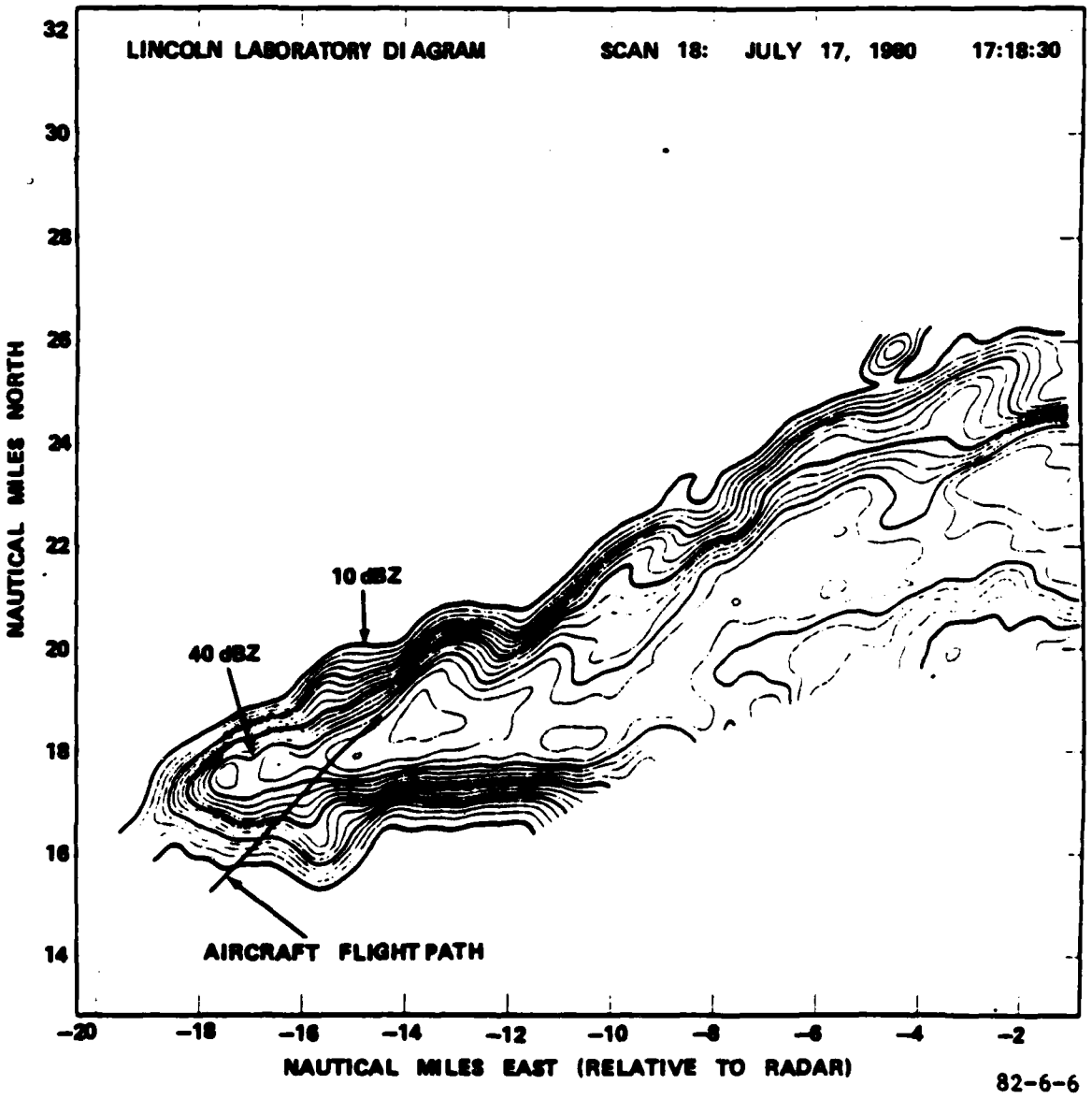

FIGURE 6. RADAR REFLECTIVITY FACTOR (PRECIPITATION INTENSITY) CONTOURS IN STEPS OF 2.5 dBZ

C = universal constant (1.77)

V = true airspeed

ρ = air density

M = aircraft mass

C_{L_α} = wing lift curve slope

S = wing area

$\epsilon_a^{1/3}$ was computed from 0.25-second preaveraged accelerations (five values) by continuously averaging over a 7.5-second period using a cosine squared weighting. $\epsilon_a^{1/3}$ values were produced each second.

3. $\epsilon_\rho^{1/3}$ from airspeed (Pitot pressure) fluctuations (reference 5).

$$\epsilon_\rho^{1/3} = \frac{\sqrt{D_V}}{C^{1/2}\, r^{1/3}} \left(cm^{2/3} sec^{-1}\right) \qquad (5)$$

where,

D_V = airspeed structure function — average of the square of the differences between successive airspeeds measured a distance r apart (homogeneous isotropic turbulence assumed)

C = Universal constant (1.77)

$\epsilon_\rho^{1/3}$ was computed from 0.2-second preaveraged Pitot pressures (20 values) by continuously averaging over a 7.5-second period using a cosine squared weighting. $\epsilon_\rho^{1/3}$ values were produced each second.

$\epsilon_a^{1/3}$ and $\epsilon_\rho^{1/3}$ are highly correlated. For a flight made on July 17, 1980, when the aircraft made several penetrations of a VIP level 4 thunderstorm, the correlation coefficient was 0.93. This was based on 497 independent consecutive 7-second data points (2/3 km air travel). For a flight made on July 16, 1980, when the aircraft made penetrations of VIP level 3 thunderstorms, the correlation was 0.91 for 521 data points. Both regression line slopes were approximately 0.75, which is consistent with MacCready (reference 7) who showed that turbulence energy measured by an aircraft longitudinally should be three-quarters of that measured vertically.

The two aircraft turbulence measurements were combined for further analysis by the following equation:

$$\epsilon_{a\rho}^{1/3} = \sqrt{\frac{\epsilon_a^{2/3} + (1.333\epsilon_\rho^{1/3})^2}{2}} \qquad (6)$$

AIRCRAFT TURBULENCE SCALES.

Peak U_{de} has been established by the NSSL to classify the degree of turbulence experienced by aircraft (references 2 and 9). The scale is:

Light: $\overline{>}$5-20 feet per second (ft/s) (1.5 - 6.1 meters per second (m/s))

Moderate: $\overline{>}$20-35 ft/s (6.1 - 10.7 m/s)

Severe: $\overline{>}$35-50 ft/s (10.7 - 15.2 m/s)

Extreme: $\overline{>}$50 ft/s (15.2 m/s)

A corresponding scale for $\epsilon_{a\rho}^{1/3}$ was determined at the Technical Center but with the U_{de} light category further classified into N = negligible (0 to 3 m/s) and L = light (3 to 6.1 m/s). The remaining categories are abbreviated: M = moderate, S = severe, and E = extreme. The $\epsilon_{a\rho}^{1/3}$ scale was tentatively established with data from the flight of July 17, 1980, when the aircraft made several penetrations of a VIP level 4 (46 to 50 dBZ, very heavy) thunderstorm. The $\epsilon_{a\rho}^{1/3}$ scale was determined by computing λ from the minimum of the following function over the data set:

$$\text{mean square error} = \frac{\Sigma(\epsilon_{a\rho}^{1/3} - \lambda U_{de})^2}{N} \qquad (7)$$

where N = number of data pairs. This was achieved by taking the partial derivative with respect to λ and setting it equal to zero.

The factor lambda was found to be 0.7. This was applied to the U_{de} category limits to determine the corresponding $\epsilon_{a\rho}^{1/3}$ category limits, except that the upper limit of the severe category was set at 12.5 to correspond to the MacCready $\epsilon^{1/3}$ upper limit for an aircraft travelling at 200 miles per hour (mph) (reference 7). The Gulfstream made penetrations at about 200 mph. This provided a more consistent gradation from the light to moderate to severe categories. The established $\epsilon_{a\rho}^{1/3}$ categories are a refinement of those determined previously from the same data (reference 10).

Table 1 shows the comparison between U_{de} and $\epsilon_{a\rho}^{1/3}$ for independent data points taken at 7-second intervals (2/3 km air travel) for the July 17, 1980, flight. The general distribution of turbulence for this storm agreed well with recorded voice comments by the pilot.

The full MacCready 200-mph $\epsilon^{1/3}$ categories (reference 7) are the following: negligible (0 to 0.8), light (0.8 to 2.2), moderate (2.2 to 5.2), severe (5.2 to 12.5), extreme ($\overline{>}$12.5). For the July 17, 1980, flight, this scale showed considerably less negligible and light turbulence and considerably more moderate and severe turbulence than the $\epsilon_{a\rho}^{1/3}$ scale. The latter is considered more realistic. The

MacCready 200-mph scale was used in a previous investigation (reference 11), and also over-observed moderate and severe turbulence relative to a scale based on airspeed fluxuations. The airspeed scale was consistent with pilot comments on turbulence severity.

The correspondence between U_{de} and $\epsilon_{a\rho}^{1/3}$ was similar to that shown by table 1 for penetrations into VIP level 3 (41 to 46 dBZ, heavy) thunderstorms on July 16, 1980, although very little severe turbulence was encountered during these penetrations. The July 16 correlation coefficient was 0.90 for 521 data points (data not shown).

TABLE 1. PEAK U_{de} VERSUS $\epsilon_{a\rho}^{1/3}$ FOR FLIGHT OF JULY 17, 1980

		$\epsilon_{a\rho}^{1/3}$ ($cm^{2/3}sec^{-1}$)					
		0 to 2.1	2.1 to 4.3	4.3 to 7.5	7.5 to 12.5	≥12.5	Total
Ude (m/s)		N	L	M	S	E	
0 to 3	N	192	32	0	0	0	224
3 to 6.1	L	10	92	39	1	0	142
6.1 to 10.7	M	0	15	66	12	0	93
10.7 to 15.2	S	0	1	14	17	1	33
≥15.2	E	0	0	2	5	0	7
Total		202	140	121	35	1	499

Correlation coefficient = 0.91

Note: Turbulence categories: N = negligible
L = light
M = moderate
S = severe
E = extreme

COMPARISON OF RADAR AND AIRCRAFT DATA.

Plots of $\epsilon_a^{1/3}$ (aircraft) and $\epsilon_r^{1/3}$ (radar) for the flight of July 17, 1980, are shown in figure 7. The radar scan numbers are entered on the radar (lower) graph. $\epsilon_r^{1/3}$ was plotted for all observed values. In subsequent processing, those values less than two were rejected because the spectrum width algorithms are considered unreliable below this threshold. However, almost all $\epsilon_r^{1/3}$ values eliminated were associated with light or negligible aircraft turbulence.

Lincoln Laboratory performed a spectral analysis of certain scans which showed that aircraft signal contamination occurred in scans 11, 30, and 39. Data from these scans were removed in subsequent processing.

The large radar peak at 17:05 was found to have a double maximum spectrum, and that near 17:30, a flat-topped spectrum. The pulse-pair algorithm will produce excessive width estimates with such non-Gaussian spectra. However, these points and others were not removed since a discriminating algorithm for such spectra has not been developed.

The correlation between radar and aircraft curves is reasonably good, although the radar curve is smoother and does not show the detailed fluctuations of the aircraft curve. A particularly good sequence is for the 17:09 to 17:15 period where the correlation coefficient between $\epsilon_{a\rho}^{1/3}$ and $\epsilon_r^{1/3}$ was 0.81. The $\epsilon_{a\rho}^{1/3}$ versus radar reflectivity factor (dBZ) correlation for the same period was 0.57.

The corresponding correlation coefficients for the entire July 17 flight were 0.51 and 0.36, respectively, for 259 data points. The correlations for the July 16 flight were 0.54 and 0.44, respectively, for 265 data points. In all correlations, the maximum radar values observed in the independent 7-second periods were used for comparison with the aircraft values.

The low overall correlations between radar and aircraft turbulence are considered to be due to several factors. One is that the aircraft more realistically measures the actual turbulence fluctuations as shown by figure 7. Other factors are the effect of the non-Gaussian spectra and deficiencies in the pulse-pair algorithm which tends to have increasing error with increasing spectral width. Wind shear could also broaden spectra, but its contribution is generally thought to be small (reference 12). Finally, errors may occur through interpolation of radar values along the aircraft track between the 80-second radar scans. These would tend to reduce the $\epsilon_r^{1/3}$ correlations more than the radar reflectivity factor (dBZ) correlations because of the more highly structured nature of $\epsilon_r^{1/3}$.

SMOOTHING OF RADAR AND AIRCRAFT DATA.

The radar and aircraft curves of figure 7 were filtered with a Gaussian-shaped filter. The filtering program used the overlap-add method of fast convolution to implement the filter. The width of the filter response in time was 300 data points (300 seconds). This width corresponds to the 1-sigma value of the Gaussian response. The radar peaks near scans 11, 30, and 39 of figure 7, which were contaminated by aircraft signal, were removed prior to the Gaussian smoothing.

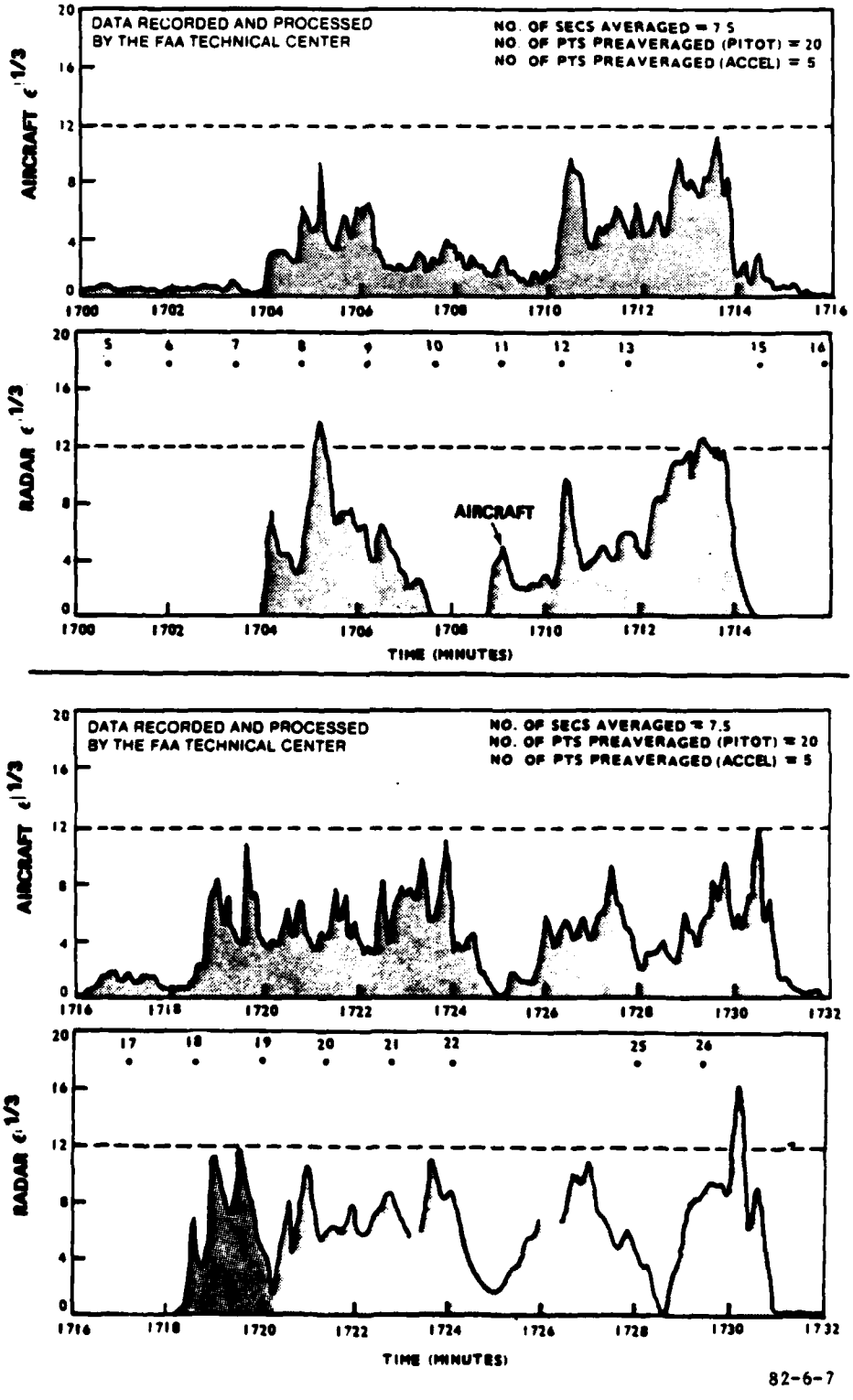

FIGURE 7. COMPARISON OF $\epsilon_{ap}^{1/3}$ AND $\epsilon_{r}^{1/3}$ FOR FLIGHT OF JULY 17, 1980

Figure 8 shows the smoothed plots for the entire flight of July 17, 1980. There is close agreement between the two curves with most sequences of turbulence coinciding in position. Amplitude-wise, the radar peaks are generally higher. The comparison indicates that with a refinement in the radar processing, particularly with respect to the wider spectra (higher turbulence levels), greater agreement could be achieved.

RADAR/AIRCRAFT TURBULENCE CATEGORIES.

The basic relationship between radar and aircraft turbulence shown by the curves of figures 7 and 8, can also be shown by classifying unsmoothed radar turbulence by category in relation to categorical aircraft turbulence (table 1). The radar categories were chosen to provide a reasonable discrimination between the classes of turbulence. The minimum function technique (equation 7) was tried to derive the radar category limits, but did not produce radar categories that associated as well with aircraft turbulence.

Table 2 shows the comparison for the July 17, 1980, flight. The information contained in table 2 is a refinement of that determined previously (reference 10). Although there is considerable mismatch in the turbulence category totals, the aircraft turbulence clearly increases up through the radar severe turbulence category. This distribution appears consistent with the character of the pulse-pair processing method. The best relationships are in the radar N and L categories, as shown by the strong association with the lower aircraft turbulence categories and the field of 0's in the higher aircraft categories. The pulse-pair algorithms are more accurate with narrow spectra, i.e., low turbulence (reference 6). Thus, when the radar signified low turbulence, the aircraft-derived turbulence was also low. With wider spectra, errors in radar spectrum width or velocity variance estimation and $\epsilon_r^{1/3}$ values increase. Also, some of the very large values of $\epsilon_r^{1/3}$ are due to non-Gaussian spectra, as noted previously.

These factors would contribute to the association of higher categories of $\epsilon_r^{1/3}$ with several categories of aircraft turbulence and give table 2 the appearance of a lower triangular distribution.

SIMPLIFIED RADAR/AIRCRAFT TURBULENCE CATEGORIES.

Table 2 was simplified in order to better illustrate the radar/aircraft turbulence relationships. The five $\epsilon_r^{1/3}$ categories of the table were reduced to three by combining the first two into LITE, and the last two into SEV, leaving the moderate category as is. The two highest $\epsilon_{ao}^{1/3}$ categories were combined into severe; the others were left as is. The results are shown in table 3. The percentages on the right are the occurrences of the indicated combined aircraft categories for the three radar categories (LITE, MOD, SEV). Table 3 shows that almost all $\epsilon_r^{1/3}$ values less than 4.5 were associated with light or no turbulence. For radar values in the 4.5 to 7 range, occurrences were concentrated in the aircraft LIGHT and MOD categories, with only four occurrences of SEV. When $\epsilon_r^{1/3}$ was ≥ 7, turbulence was mostly moderate to severe, with the occurrence of severe increasing sharply. The corresponding data for the flight of July 16 are shown in table 4. Here we see

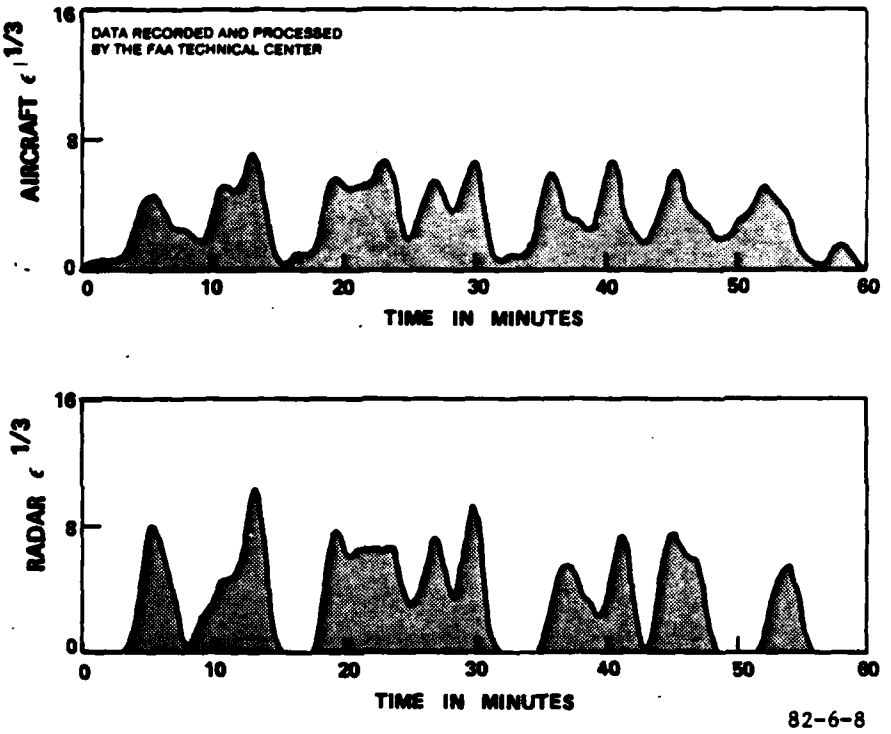

FIGURE 8. COMPARISON OF $\epsilon_{a\rho}^{1/3}$ AND $\epsilon_{r}^{1/3}$ FOR FLIGHT OF JULY 17, 1980 AFTER SMOOTHING

TABLE 2. $\epsilon_{r}^{1/3}$ VERSUS $\epsilon_{a\rho}^{1/3}$ FOR FLIGHT OF JULY 17, 1980

		$\epsilon_{a\rho}^{1/3}$ ($cm^{2/3}sec^{-1}$)					
		0 to 2.1	2.1 to 4.3	4.3 to 7.5	7.5 to 12.5	≥12.5	Total
$\epsilon_{r}^{1/3}$		N	L	M	S	E	
2 to 3	N	10	10	0	0	0	20
3 to 4.5	L	10	25	6	0	0	41
4.5 to 7	M	11	34	42	4	0	91
7 to 12.5	S	6	17	49	25	1	98
≥12.5	E	1	3	3	2	0	9
Total		38	89	100	31	1	259

Correlation coefficient = 0.51

Note: Turbulence categories: N = negligible, L = light, M = moderate, S = severe, E = extreme.

TABLE 3. $\epsilon_r^{1/3}$ VERSUS $\epsilon_{ap}^{1/3}$ FOR FLIGHT OF JULY 17, 1980 (SIMPLIFIED)

	$\epsilon_{ap}^{1/3}$ NEG	LIGHT	MOD	SEV			
$\epsilon_r^{1/3}$	0 to 2.1	2.1 to 4.3	4.3 to 7.5	≥7.5	Total	Comb. Cat.	%
LITE (2 to 4.5)	20	35	6	0	61	N-L	90
MOD (4.5 to 7)	11	34	42	4	91	L-M	84
SEV (≥7)	7	20	52	28	107	M-S	75
Total	38	89	100	32	259		

Correlation coefficient = 0.51

TABLE 4. $\epsilon_r^{1/3}$ VERSUS $\epsilon_{ap}^{1/3}$ FOR FLIGHT OF JULY 16, 1980 (SIMPLIFIED)

	$\epsilon_{ap}^{1/3}$ NEG	LIGHT	MOD	SEV			
$\epsilon_r^{1/3}$	0 to 2.1	2.1 to 4.3	4.3 to 7.5	≥7.5	Total	Comb. Cat.	%
LITE (2 to 4.5)	58	61	11	0	130	N-L	92
MOD (4.5 to 7)	28	43	24	0	95	L-M	71
SEV (≥7)	3	10	23	4	40	M-S	68
Total	89	114	58	4	265		

Correlation coefficient = 0.54

similar relationships, though not as discriminating in the $\epsilon_r^{1/3}$ MOD and SEV categories.

CONSIDERATION OF RADAR REFLECTIVITY FACTOR.

Correlation coefficients between radar reflectivity factor (dBZ) and the aircraft turbulence measures are approximately 0.4. This indicates that dBZ has some value as a turbulence predictor. Consequently, table 3 was divided into two tables according to the association of $\epsilon_r^{1/3}$ with dBZ $\geq$35 and <35. The screened distributions are shown in tables 5 and 6, respectively.

Table 5 shows the cases for $\epsilon_r^{1/3}$ with dBZ $\geq$35, and table 6 for the cases with dBZ <35. Table 5 shows an enhanced relationship for $\epsilon_r^{1/3}$ in the SEV category, about the same association for MOD, and a slight degradation for LITE. On the other hand, table 6 shows a much degraded association for $\epsilon_r^{1/3}$ values in the SEV category, about the same for MOD, and a slight improvement for LITE. Note that no aircraft severe turbulence occurred in the $\epsilon_r^{1/3}$ SEV category, all cases being associated with dBZ $\geq$35. This difference was primarily responsible for the spread in correlation coefficients (0.59 versus 0.30).

Similar results were obtained for the July 16 mission with correlation coefficients of 0.68 and 0.30, respectively, for dBZ $\geq$35 and <35. The overall correlation coefficient was 0.54. The tendency for the association of high turbulence with high radar reflectivity factor was also noted for other research flights into thunderstorms (discussed in reference 11).

TABLE 5. $\epsilon_r^{1/3}$ VERSUS $\epsilon_{a\rho}^{1/3}$ FOR dBZ $\geq$35 (JULY 17, 1980)

	$\epsilon_{a\rho}^{1/3}$						
$\epsilon_r^{1/3}$	NEG 0 to 2.1	LIGHT 2.1 to 4.3	MOD 4.3 to 7.5	SEV $\geq$7.5	Total	Comb. Cat.	%
LITE (2 to 4.5)	11	14	5	0	30	N-L	83
MOD (4.5 to 7)	7	25	24	3	59	L-M	83
SEV ($\geq$7)	1	10	39	28	78	M-S	86
Total	19	49	68	31	167		

Correlation coefficient = 0.59

TABLE 6. $\epsilon_r^{1/3}$ VERSUS $\epsilon_{a\rho}^{1/3}$ FOR dBZ <35 (JULY 17, 1980)

$\epsilon_r^{1/3}$	$\epsilon_{a\rho}^{1/3}$ NEG 0 to 2.1	LIGHT 2.1 to 4.3	MOD 4.3 to 7.5	SEV ≥7.5	Total	Comb. Cat.	%
LITE (2 to 4.5)	9	21	1	0	31	N-L	97
MOD (4.5 to 7)	4	9	18	1	32	L-M	84
SEV (≥7)	6	10	13	0	29	M-S	45
Total	19	40	32	1	92		

Correlation coefficient = 0.30

SUMMARY OF RESULTS

1. Aircraft turbulence measurements in terms of $\epsilon^{1/3}$ (turbulence dissipation factor) agree well with peak U_{de} (derived gust velocity), an established aircraft turbulence measure. Categories of aircraft turbulence in terms of $\epsilon^{1/3}$ were determined through the relationship.

2. Radar $\epsilon^{1/3}$ correlates better with aircraft $\epsilon^{1/3}$ than does radar reflectivity factor. For one 6-minute sequence during penetration of a very heavy thunderstorm, the correlation coefficient was 0.81 for radar $\epsilon^{1/3}$ versus aircraft $\epsilon^{1/3}$, and 0.57 for radar reflectivity factor versus aircraft $\epsilon^{1/3}$. The overall correlations for several penetrations of very heavy and heavy thunderstorms were about 0.5 for radar versus aircraft $\epsilon^{1/3}$, and 0.4 for radar reflectivity factor versus aircraft $\epsilon^{1/3}$. The low overall correlation coefficients between radar and aircraft $\epsilon^{1/3}$ are considered to be due to differences in the two measuring systems, deficiencies in the radar processing, and radar data interpolation errors between the 80-second radar scans.

3. Despite the low overall correlation, plots of the data showed a basic relationship between radar and aircraft turbulence. This was illustrated more clearly by a smoothing technique that removed the high frequency components from the data sets. The result was a close matchup in the sequences of turbulence observed by both radar and aircraft.

4. In penetrations of a very heavy thunderstorm, about 90 percent of the radar values less than 4.5 (classified as light turbulence) were associated with negli-

gible or light aircraft turbulence and none with severe. About 85 percent of the radar values between 4.5 and 7 (classified as moderate turbulence) were associated with light and moderate aircraft turbulence. Only about 5 percent were associated with severe. Radar $\epsilon_r^{1/3}$ values equal to or greater than 7 (classified as severe turbulence) were mostly associated with moderate and severe aircraft turbulence (about 75 percent). Results were analogous for penetrations of heavy thunderstorm cells where very little severe turbulence was observed.

5. In penetrations of the very heavy thunderstorm, about 85 percent of the radar $\epsilon_r^{1/3}$ values equal to or greater than 7 (severe turbulence) were associated with moderate and severe aircraft turbulence when the radar reflectivity factor was equal to or greater than 35 dBZ. (This compares with 75 percent for all dBZ values, see item 4.) When the radar reflectivity factor was less than 35 dBZ, only about 45 percent of the radar $\epsilon_r^{1/3}$ values ≥ 7 were associated with moderate turbulence, with no aircraft severe turbulence being observed. Results were analogous for penetrations of the heavy thunderstorm cells.

CONCLUSIONS

1. A pulse Doppler radar system can make reasonably accurate observations of thunderstorm turbulence in terms of $\epsilon^{1/3}$ (turbulence dissipation factor).

2. Radar $\epsilon^{1/3}$, classified into light, moderate, and severe turbulence categories, is a potentially useful predictor of thunderstorm turbulence.

3. The predictive value of the radar $\epsilon^{1/3}$ turbulence categories is enhanced when used in combination with radar reflectivity factor categories of 35 dBZ and above, and below 35 dBZ.

RECOMMENDATIONS

1. Continue data collection.

2. Increase radar sampling time to minimize radar data interpolation errors between scans.

3. Improve measurement of radar $\epsilon^{1/3}$ through more accurate spectral width estimation.

REFERENCES

1. Burnham, J., and Lee, J. T., Thunderstorm Turbulence and its Relationship to Weather Radar Echoes, J. Aircraft, 6, 1969, pp. 438-455.

2. Lee, J. T., Thunderstorm Turbulence, Proc. FAA Turbulence Symposium, Washington, D.C., 1971.

3. Spahn, J. F., and Smith, P. L., Some Characteristics of Hailstone Size Distributions Inside Hailstorms, Preprints 17th Conf. on Radar Meteorology, Amer. Meteor. Soc., Boston, 1976.

4. Oliver, R. G., Design of an Improved Weather Contouring Device, Report No. FAA-RD-80-6, FAA Systems Research and Development Service, Washington D.C., 1980.

5. Labitt, M., Coordinated Radar and Aircraft Observations of Turbulence, Report ATC-108, Massachusetts Institute of Technology, Lincoln Laboratory, Lexington, Mass. (prepared for FAA Systems Research and Development Service), 1981.

6. Advances in Radar Meteorology (an Intensive Short Course) Lecture VI (D. Zrnic'), Technology Service Corp., Silver Spring, Md., 1981.

7. MacCready, P. B. Jr., Standardization of Gustiness Values from Aircraft, J. Appl. Meteorology, 3, 1964, pp. 439-449.

8. Crooks, W., High Altitude Clear Air Turbulence, Report No. AFFDL-TR-65-144, AF Flight Dynamics Laboratory, Air Force Systems Command, Wright-Patterson AFB, Ohio, 1965.

9. National Air Traffic Training Program, Flight Service, Phase 5; The Preflight Position, Department of Transportation, FAA Aeronautical Center, Oklahoma City, Vol. 1, June 27, 1972, pp. 2-26.

10. Lewis, W., Doppler Radar and Aircraft Measurements of Thunderstorm Turbulence, Preprints 20th Conference on Radar Meteorology, American Meteorological Society, Boston, Mass., 1981.

11. Sand, W. R., Musil, D. J., and Kyle, T. G., Observations of Turbulence and Icing Inside Thunderstorms, Preprints 6th Conf. on Aerospace and Aeronautical Meteorology, Amer. Meteor. Soc., Boston, Mass., 1974.

12. Doviak, R. J., Sirmans, D., Zrnic, D., and Walker, G. B., Considerations for Pulse-Doppler Radar Observations of Severe Thunderstorms, J. Appl. Meteorology, 17, 1978, pp. 189-205.

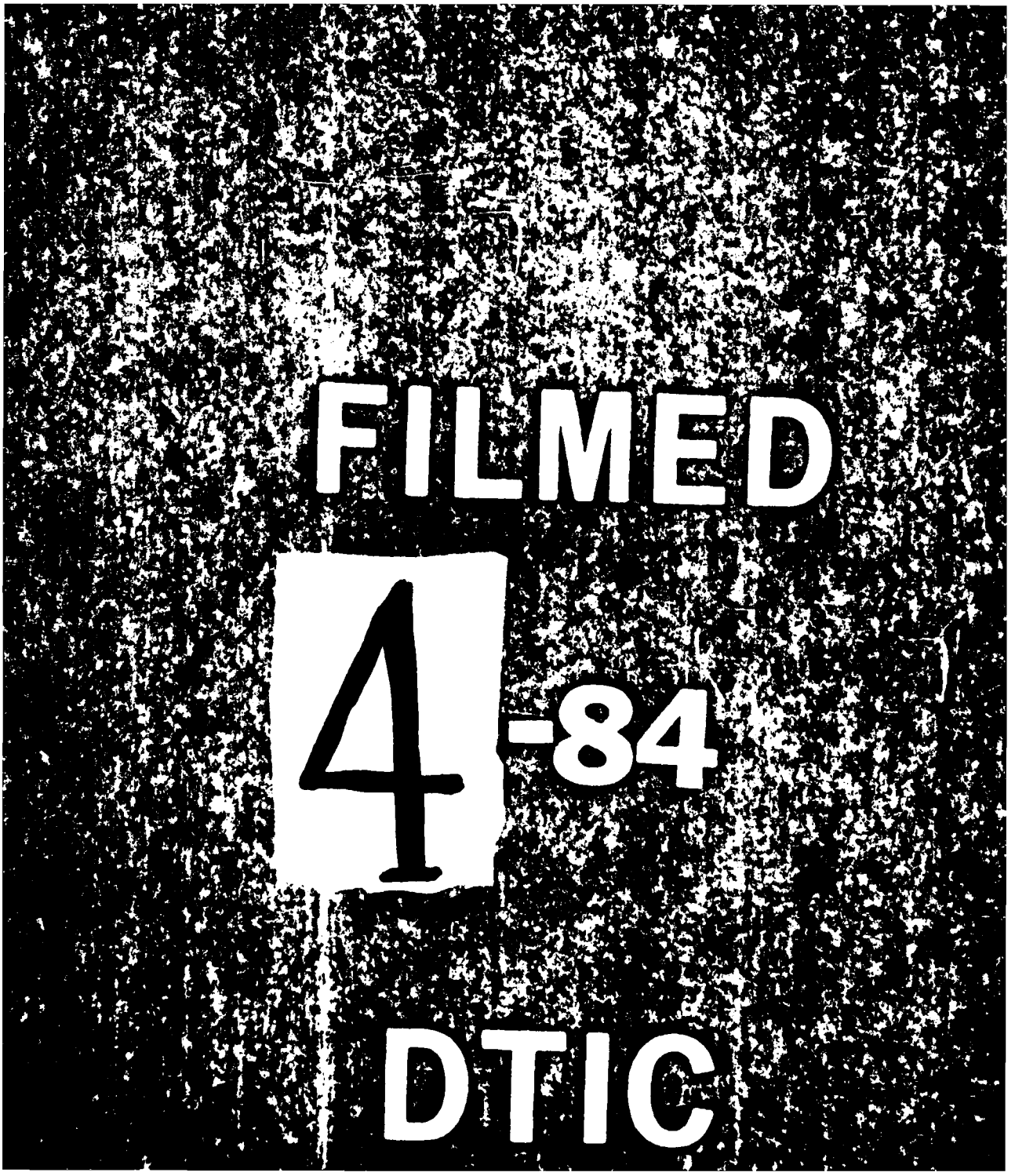
FILMED
4-84
DTIC